

Thickness of the strangelet-crystal crust of a strange star

Mark G. Alford and David A. Eby

Physics Department, Washington University, St. Louis, MO 63130, USA

(Dated: 5 August 2008)

It has recently been pointed out that if the surface tension of quark matter is low enough, the surface of a strange star will be a crust consisting of a crystal of charged strangelets in a neutralizing background of electrons. This affects the behavior of the surface, and must be taken into account in efforts to observationally rule out strange stars. We calculate the thickness of this “mixed phase” crust, taking into account the effects of surface tension and Debye screening of electric charge. Our calculation uses a generic parametrization of the equation of state of quark matter. For a reasonable range of quark matter equations of state, and surface tension of order a few MeV/fm², we find that the preferred crystal structure always involves spherical strangelets, not rods or slabs of quark matter. We find that for a star of radius 10 km and mass $1.5M_{\odot}$, the strangelet-crystal crust can be from zero to hundreds of meters thick, the thickness being greater when the strange quark is heavier, and the surface tension is smaller. For smaller quark stars the crust will be even thicker.

PACS numbers: 25.75.Nq, 26.60.+c, 97.60.Jd

I. INTRODUCTION

Quarks in their most familiar form are confined in protons and neutrons that make up standard nuclear matter. However, according to the “strange matter hypothesis” [1, 2] this form of matter might be metastable and the fully stable state would then be “strange matter”, which contains roughly equal numbers of up, down, and strange quarks. Large (kilometer-sized) pieces of strange matter are “strange stars” (for a review see Ref. [3]); small nuggets of strange matter are “strangelets” [4]. The strange matter hypothesis remains a fascinating but unproven conjecture. In this paper we will assume that it is correct, and investigate the structure of the crust of a strange star.

The traditional picture of the surface of a strange star is a sharp interface, of thickness ~ 1 Fermi. Below the interface lies quark matter, the top layer of which is positively charged. Above the interface is a cloud of electrons, sustained by an electric field which could also support a thin nuclear matter crust in suspension above the quark matter [5, 6], as long as the strange star is not too hot [7].

However, if the surface tension σ of the interface between quark matter and the vacuum is small enough, the surface will take on a much more complicated structure. If σ is less than a critical value σ_{crit} then large lumps of strange matter are unstable against fission into smaller pieces [8, 9]. As a result, the simple surface described in the previous paragraph is unstable, and is replaced by a mixed phase involving nuggets of positively-charged strange matter in a neutralizing background of electrons. It is reasonable to guess that the ground state is a regular lattice, leading to a crust with a crystalline structure. (Note that this crystal is completely different from the Larkin-Ovchinnikov-Fulde-Ferrell phase of quark matter [10, 11], where the quark matter density is uniform, but the pairing gap varies in space.) Jaikumar, Reddy, and Steiner [8] conjecture that the strangelet crystal crust will

actually be a multi-layer structure of mixed phases, analogous to the “nuclear pasta” phases that occur in models of the inner crust of a conventional neutron star [12]. At the outer edge of the crust, we expect a dilute low-pressure lattice of small strangelets in a degenerate gas of electrons. As we descend in to the star, the pressure rises, and the structure is modified (becoming denser, and perhaps changing to rods, slabs, cavities, etc). At a critical pressure p_{crit} the mixed phase is no longer stable, and there is a transition to uniform neutral quark matter. As one burrows deeper into the star the pressure continues to rise, and there may be other phase transitions between different phases of quark matter [13], but those will not concern us here. Note that in this scenario the strange star depends on gravity for its existence. In the absence of gravity, it would undergo fission into strangelets.

Ref. [8], assuming zero surface tension and neglecting Debye screening, estimated that the mixed phase crust might be 40 – 100 m thick, with $p_{\text{crit}} \approx 1000$ MeV⁴. This is an interesting result because if a strange star has a sufficiently thick crystalline crust, it might be hard to distinguish from the crust of a neutron star. Astrophysical properties that are sensitive to the crust include cooling behavior, neutrino and photon opacity during a supernova, the photon emission spectrum, glitches, and frequencies of seismic vibrations which are observed after giant flares in magnetars. For further discussion and references see Sec. VI. This paper will make a more careful calculation of the properties of a strangelet crystal crust, including the effects of Debye screening [14] and surface tension.

We expect that the properties of the crust will emerge from a competition between various different contributions to the energy. Charge separation is often favored by the internal energy of the phases involved, because a neutral phase is always a maximum of the free energy with respect to the electrostatic potential (see [12, 15]; for a pedagogical discussion see [16]). The domain struc-

ture is determined by surface tension (which favors large domains) and electric field energy (which favors small domains). Debye screening is important because it redistributes the electric charge, concentrating it in the outer part of the quark matter domains and the inner part of the surrounding vacuum, and thereby modifying the internal energy and electrostatic energy contributions.

To make an estimate of the thickness of the crust we need to calculate the equation of state of the mixed phase, i.e. the energy density ε_{mp} as a function of the pressure p_{mp} . The thickness of the crust for a star of mass M is then

$$\Delta R = R_{\text{star}} \left(\frac{R_{\text{star}}}{GM} - 2 \right) \int_0^{p_{\text{crit}}} \frac{1}{\varepsilon_{\text{mp}}} dp_{\text{mp}}, \quad (1)$$

in $\hbar = c = 1$ units. This expression follows from the Tolman Oppenheimer Volkoff equation [17, 18], assuming that $\Delta R \ll R_{\text{star}}$, and that everywhere in the crust the pressure is much smaller than both the local energy density and the average energy density of the whole star. These are very good approximations for the cases that we study.

We obtain ε_{mp} as a function of p_{mp} by dividing the strangelet lattice into unit cells (“Wigner-Seitz cells”) and calculating the pressure at the edge of a cell as a function of its energy density. We study cells that are three-dimensional (a lattice of strangelets in a degenerate gas of electrons), two-dimensional (rods of strange matter in a degenerate gas of electrons) and one-dimensional (slabs of strange matter interleaved with regions of degenerate electron gas). Our approach is similar to that used in studying mixed phases of quark matter and nuclear matter in the interior of neutron stars [19].

We build on the formalism for a generic quark matter equation of state and infinitely-large Wigner-Seitz cells that was developed in [8, 9]. The main assumptions that we make are:

- 1) Within each Wigner-Seitz cell we use a Thomas-Fermi approach, solving the Poisson equation to obtain the charge distribution, energy density, and pressure. This is incorrect for very small strangelets, where the energy level structure of the quarks becomes important [20, 21]; such corrections may be relevant for the very low pressure (outer crust) part of our results (see Sec. VI).
- 2) We assume our D -dimensional Wigner-Seitz cells to be D -spheres. In reality the cells will be unit cells of some regular lattice (cubic, hexagonal close packed, etc). However, as long as the cell is much bigger than the strangelet inside it, we expect this approximation to be reasonably accurate. We will only report results for cases where $R_{\text{cell}} > 2R$ (R being the radius of the quark matter in the center of the cell, which we expect will have a rotationally symmetric shape because of the surface tension). In some cases this assumption is violated, and we will then only be able to obtain a lower limit on the crust thickness (see Sec. VB 2).
- 3) We treat the interface between quark matter and the vacuum as a sharp interface, with no charge localized on

it, which is characterized by a surface tension. We neglect any surface charge that might arise from the reduction of the density of states of strange quarks at the surface [22, 23, 24, 25]. We also neglect the curvature energy of a quark matter surface [26, 27], so we do not allow for “Swiss-cheese” mixed phases, in which the outer part of the Wigner-Seitz cell is filled with quark matter, with a cylindrical or spherical cavity in the center, for which the curvature energy is crucial. Note that these phases would be expected to occur at higher pressure than the ones we study, so including them is likely to make the crust even thicker than we predict.

- 4) We assume that the chemical potential for negative electric charge μ_e is much less than the chemical potential for quark number μ . This allows us to expand the quark matter equation of state in powers of μ_e , and means that within the quark matter we can ignore the contribution of electrons to the charge and pressure. This is a very good approximation for small strange quark mass, which corresponds to small n_Q in our parameterization. For the largest value of n_Q that we study, μ_e in neutral quark matter is close to 100 MeV, and the assumption is still reasonable.
- 5) We assume that only electrons are present, with no muons. This is valid as long as μ_e is less than the muon mass m_μ , which is true for all the cases that we study.
- 6) We assume that μ_e is always much greater than the electron mass. Thus in the degenerate electron gas, we can take the electrons to be massless, which simplifies the Thomas-Fermi calculation of their charge distribution. Since μ_e drops monotonically from the center of the cell to its edge, this condition will only be violated for very large cells (very low pressures).
- 8) We always work at zero temperature. The temperature of the surface of a compact star, even during a flare [28], is expected to be less than 100 keV, so we expect this to be a reasonable approximation.

II. CHARACTERIZATION OF QUARK MATTER

A. Generic parametrization

We use the generic parametrization of the quark matter equation of state suggested in Ref. [9],

$$p_{\text{QM}}(\mu, \mu_e) = p_0(\mu) - n_Q(\mu)\mu_e + \frac{1}{2}\chi_Q(\mu)\mu_e^2 + \dots \quad (2)$$

which expresses the pressure as a function of the chemical potential for quark number (μ) and for negative electric charge (μ_e), expanded to second order in μ_e . In addition, we assume that there is a surface tension σ associated with the interface between quark matter and vacuum. In this paper we do not include curvature energy.

This parametrization is model-independent. Any specific model of quark matter can be represented by appropriate choices of σ , p_0 , the charge density n_Q , and charge susceptibility χ_Q .

The quark density n and the electric charge density q_{QM} (in units of the positron charge) are

$$n = \frac{\partial p_{\text{QM}}}{\partial \mu}, \quad q_{\text{QM}} = -\frac{\partial p_{\text{QM}}}{\partial \mu_e} = n_Q - \chi_Q \mu_e. \quad (3)$$

So in uniform neutral quark matter the electron chemical potential is $\mu_e^{\text{neutral}} = n_Q/\chi_Q$. Eq. (2) is a generic parametrization if $\mu_e^{\text{neutral}} \ll \mu$, which is typically the case in three-flavor quark matter.

The bag constant enters in $p_0(\mu)$, and we will fix it by requiring that the first-order transition between neutral quark matter and the vacuum occur at quark chemical potential μ_{crit} , i.e. $p(\mu_{\text{crit}}, \mu_e^{\text{neutral}}) = 0$. Because we are assuming that the strange matter hypothesis is valid, we must have $\mu_{\text{crit}} \lesssim 310$ MeV, since at $\mu \approx 310$ MeV there is a transition from vacuum to neutral nuclear matter. In this paper we will typically use $\mu_{\text{crit}} = 300$ MeV. The value of μ inside our quark matter lumps will always be very close to μ_{crit} , so we can evaluate n_Q and χ_Q at μ_{crit} , and not be concerned about their μ -dependence.

We will restrict ourselves to values of the surface tension that are below the critical value [9]

$$\sigma_{\text{crit}} = 0.1325 \frac{n_Q^2 \lambda_D}{\chi_Q} = 0.1325 \frac{n_Q^2}{\sqrt{4\pi\alpha\chi_Q}^{3/2}}, \quad (4)$$

where $\alpha = 1/137$ and λ_D is the Debye length

$$\lambda_D = \frac{1}{\sqrt{4\pi\alpha\chi_Q}}. \quad (5)$$

For typical models of quark matter, σ_{crit} is of order 1 to 10 MeV/fm² (see Table I). If the surface tension is larger than σ_{crit} then the energetically favored structure for the crust will not be a strangelet crystal but the simple sharp surface that has been assumed in the past [5, 7].

B. Specific equations of state

When we show numerical results we will need to vary n_Q and χ_Q over a range of physically reasonable values. To give a rough idea of what values are appropriate, we consider the example of non-interacting three-flavor quark matter, for which n_Q and χ_Q become functions of μ and the strange quark mass m_s , while p_0 is in addition a function of the bag constant B . Expanding to lowest non-trivial order in m_s ,

$$\begin{aligned} p_0(\mu) &= \frac{9\mu^4}{12\pi^2} - B, \\ n_Q(\mu, m_s) &= \frac{m_s^2 \mu}{2\pi^2}, \\ \chi_Q(\mu, m_s) &= \frac{2\mu^2}{\pi^2}. \end{aligned} \quad (6)$$

We emphasize that these expressions are simply meant to give a rough idea of reasonable physical values for n_Q

and χ_Q . Our treatment does not depend on an expansion in powers of m_s . To tune the transition between neutral quark matter and the vacuum so it occurs at $\mu = \mu_{\text{crit}}$ (see previous subsection), we set B so that $p_0(\mu_{\text{crit}}) = \frac{1}{2}n_Q^2(\mu_{\text{crit}})/\chi_Q(\mu_{\text{crit}})$.

In the regions between lumps of strange matter, we will assume that there is a degenerate electron gas, which we treat in the Thomas-Fermi approximation. As long as μ_e is much greater than the electron mass, we can treat the electrons as massless particles, whose pressure and charge density (in units of e) is

$$p_{e^-}(\mu_e) = \frac{\mu_e^4}{12\pi^2}, \quad q_{e^-}(\mu_e) = -\frac{\mu_e^3}{3\pi^2}. \quad (7)$$

III. ANALYSIS OF A WIGNER-SEITZ CELL

We will study one, two, and three dimensional Wigner-Seitz cells. In the center there is a slab, rod, or sphere of quark matter, with radius R . The cell itself has radius R_{cell} . We want to calculate the equation of state of a mixed phase made of Wigner-Seitz cells, so we solve for the charge density, energy density, and pressure throughout the cell, using the Thomas-Fermi approximation for the contributions of quarks and electrons. This corresponds to solving the Poisson equation, which reads (in Heaviside-Lorentz units with $\hbar = c = 1$)

$$\nabla^2 \mu_e(r) = -4\pi\alpha q(r), \quad (8)$$

where $q(r)$ is the electric charge density in units of the positron charge e , and μ_e is the electrostatic potential divided by e . The equation is not trivial to solve because the charge density is itself a function of μ_e (see (3)). The boundary conditions are that there is no electric field in the center of the cell (no δ -function charge there), and no electric field at the edge of the cell (the cell is electrically neutral),

$$\frac{d\mu_e}{dr}(0) = 0, \quad \frac{d\mu_e}{dr}(R_{\text{cell}}) = 0. \quad (9)$$

We also need a matching condition at the edge of the quark matter, i.e. at $r = R$. As discussed in Sec. I, we assume that no charge localized on the surface, so we require continuity of the potential and electric field at $r = R$,

$$\mu_e(R+\delta) = \mu_e(R-\delta), \quad \frac{d\mu_e}{dr}(R+\delta) = \frac{d\mu_e}{dr}(R-\delta). \quad (10)$$

In two or three dimensional cells, the value of μ inside the strange matter will be slightly different from μ_{crit} because the surface tension compresses the droplet. To determine the value of μ , we require the pressure discontinuity across the surface of the strangelet to be balanced by the surface tension:

$$p_{\text{QM}}(\mu, \mu_e(R)) - p_{e^-}(\mu_e(R)) = \frac{(D-1)\sigma}{R}. \quad (11)$$

Once these equations are solved, we can obtain the relevant properties of the cell. The total energy of a D -dimensional Wigner-Seitz cell is

$$\begin{aligned}
E &= \int_0^R \Omega_D(r) dr \left(\mu n(\mu_e) - \frac{1}{2} \mu_e q_{\text{QM}}(\mu_e) - p_{\text{QM}}(\mu, \mu_e) \right) \\
&+ \int_R^{R_{\text{cell}}} \Omega_D(r) dr \left(-\frac{1}{2} \mu_e q_{e^-}(\mu_e) - p_{e^-}(\mu_e) \right) \\
&+ \Omega_D(R) \sigma,
\end{aligned} \tag{12}$$

where μ_e is a function of r , and $\Omega_D(r)$ is the surface areas of a $(D-1)$ -sphere, i.e.

$$\Omega_1 = 2, \quad \Omega_2(r) = 2\pi r, \quad \Omega_3(r) = 4\pi r^2. \tag{13}$$

The $-\frac{1}{2}\mu_e q$ terms in (12) come from combining $-\mu_e q$ (from the relationship between energy density and pressure) with the electric field energy density $+\frac{1}{2}\mu_e q$. The external pressure of the cell is simply the pressure of the electrons at the edge of the cell,

$$p_{\text{ext}} = p_{e^-}(\mu_e(R_{\text{cell}})). \tag{14}$$

The total number of quarks is

$$N = \int_0^R \Omega_D(r) dr n(\mu, \mu_e). \tag{15}$$

The volume of the cell is $V = 2R_{\text{cell}}$, πR_{cell}^2 , or $(4/3)\pi R_{\text{cell}}^3$ for $D = 1, 2, 3$ respectively, because we are assuming rotationally symmetric cells.

By varying R and R_{cell} we generate a two-parameter family of strangelets. However, there is really only a single-parameter family of physical configurations, parameterized by the external pressure p_{ext} . On each line of constant p_{ext} in the (R, R_{cell}) parameter space, we must minimize the enthalpy per quark,

$$h = \frac{E + p_{\text{ext}} V}{N}, \tag{16}$$

to find the favored configuration. We are at zero temperature so h is also the Gibbs free energy per quark. This is done separately for $D = 1, 2, 3$ cells, and the structure with the lowest h is the favored one.

We now have a well-defined way to obtain the equation of state of the mixed phase of quark matter, namely the energy density $\varepsilon_{\text{mp}} = E/V$ as a function of the pressure $p_{\text{mp}} = p_{\text{ext}}$. This, via (1), determines the thickness of the strangelet crust.

IV. SOLUTIONS FOR THE WIGNER-SEITZ CELL

A. Quark matter

Inside the quark matter, we can solve the Poisson equation (8) analytically. We can rewrite it using (2) and (3)

as

$$\nabla^2 \mu_e(r) = -4\pi\alpha(n_Q - \chi_Q \mu_e(r)). \tag{17}$$

In $D = 1, 2$, or 3 , the solutions obeying the first boundary condition in (9) are

$$\begin{aligned}
\mu_{e,1D}(r) &= \frac{n_Q}{\chi_Q} + A \cosh\left(\frac{r}{\lambda_D}\right), \\
\mu_{e,2D}(r) &= \frac{n_Q}{\chi_Q} + A J_0\left(\frac{ir}{\lambda_D}\right), \\
\mu_{e,3D}(r) &= \frac{n_Q}{\chi_Q} + \frac{A}{\lambda_D r} \sinh\left(\frac{r}{\lambda_D}\right).
\end{aligned} \tag{18}$$

The function J_0 is the zeroth order Bessel function of the first kind, and it is a function of the square of its argument, so the result is always real. The integration constant A will be determined by matching to the solution outside the strange matter.

B. Electron gas

In the degenerate electron gas region outside the strange matter, from (7) and (8) the Poisson equation becomes

$$\nabla^2 \mu_e(r) = \frac{4\alpha}{3\pi} \mu_e(r)^3. \tag{19}$$

There are three ways in which we were able to solve this equation. In $D = 1$, there is an exact analytic solution, which we present below. In any number of dimensions there is an approximate analytic solution, obtained by perturbing in powers of α , which works as long as the cell is not too large. Finally, one can use brute-force numerical methods to solve the differential equations with the appropriate boundary conditions. We used all three methods, checking their agreement with each other in situations where more than one of them was applicable. In our numerical results we give the values obtained by numerical solution of the Poisson equation.

1. Analytic solution for slabs

In one dimension, the Poisson equation is

$$\frac{d^2 \mu_e}{dr^2} = \frac{4\alpha}{3\pi} \mu_e^3. \tag{20}$$

By a change of variable to $\varphi = i\sqrt{2\alpha/3\pi} \mu_e$, this becomes

$$\frac{d^2 \varphi}{dr^2} = -2\varphi^3, \tag{21}$$

which belongs to a class of differential equations whose solutions are Jacobi elliptic functions $\text{sn}(r|m)$ where m is the ‘‘parameter’’ [29]. (Some authors write this as $\text{sn}(r, k)$

where $m = k^2$ and k is the elliptic modulus.) The Jacobi elliptic function obeys

$$\frac{d^2 \text{sn}(r|m)}{dr^2} = -(1+m) \text{sn}(r|m) + 2m \text{sn}(r|m)^3, \quad (22)$$

which reduces to (21) for $m = -1$, so the closed form solution is

$$\varphi(r) = \frac{1}{X} \text{sn} \left(\frac{r - R_{\text{cell}}}{X} + iK(-1), \left| -1 \right. \right) \quad (23)$$

where X is an integration constant, to be fixed by matching to the quark matter solution at $r = R$. The argument is shifted by $iK(-1)$ to ensure that $\varphi'(R_{\text{cell}}) = 0$ (the boundary condition (9) at $r = R_{\text{cell}}$). $K(m)$ is the complete elliptic integral of the first kind, so $K(-1) \approx 1.3110288$. Then φ is purely imaginary, and undoing the change of variables, the solution for μ_e is

$$\mu_{e,1D}(r) = -i \sqrt{\frac{3\pi}{2\alpha}} \frac{1}{X} \text{sn} \left(\frac{r - R_{\text{cell}}}{X} + iK(-1), \left| -1 \right. \right). \quad (24)$$

For one-dimensional slabs of quark matter we now have a complete analytic solution, combining (18) at $r < R$ with (24) at $r > R$, with X and A fixed by (10).

2. Perturbative solution for cylinders and spheres

Another approach to solving (19), which works in any number of dimensions, is to expand in powers of the electromagnetic coupling strength α . We write

$$\mu_e(r) = \mu_0(r) + \alpha \mu_1(r) + \alpha^2 \mu_2(r) + \dots \quad (25)$$

Substituting in to (19) and identifying powers of α , we find that to order α ,

$$\nabla^2 \mu_0(r) = 0, \quad \nabla^2 \mu_1(r) = \frac{4}{3\pi} \mu_0(r)^3 \quad (26)$$

Solving these equations in $D = 2, 3$, we find

$$\begin{aligned} \mu_{e,2D}(r) &= B + C \log(r/\lambda_D) + \frac{\alpha r^2}{6\pi} \left[2B^3 - 6B^2C \right. \\ &\quad \left. + 9BC^2 - 6C^3 \right] + 3(2B^2 - 4BC + 3C^2) \log(r/\lambda_D) \\ &\quad \left. + 6(B - C)C^2 \log(r/\lambda_D)^2 + 2C^3 \log(r/\lambda_D)^3 \right], \\ \mu_{e,3D}(r) &= B - \frac{C}{r} + \frac{2\alpha}{9\pi r} \left[B^2 r^2 (9C + Br) \right. \\ &\quad \left. - 6C^2 (C - Br) \log(r/\lambda_D) \right]. \end{aligned} \quad (27)$$

In each equation, the first two terms on the right-hand side are the vacuum solution μ_0 , and the remainder are the first-order correction. The integration constants B and C , along with A from (18), are determined by the boundary condition (9) at $r = R_{\text{cell}}$ and the matching condition (10).

The perturbative solution works when screening is a small correction to the unscreened (zeroth-order) electrostatic potential. It is most reliable in three dimensions, where the zeroth-order electrostatic potential becomes small at large r . We used it to check our numerical results.

V. NUMERICAL RESULTS

To get a good estimate of how thick strange star crusts might be, we vary μ_{crit} , n_Q , and χ_Q in the quark matter equation of state (6), and the surface tension σ , over a physically reasonable range, calculating the crust thickness in each case. The results of our calculations are displayed in Tables I and II. Before discussing them, we describe how they were obtained.

A. Geometry of the mixed phase

For a given quark matter equation of state, we need to find the maximum pressure up to which a stable mixed phase exists. At each lower value of the pressure we must establish the geometric configuration of the mixed phase. We can then calculate the energy density as a function of the pressure, and obtain the crust thickness using (1).

We follow the procedure described at the end of Sec. III, varying the radius of the cell R_{cell} and the radius R of the quark matter region at its center, to find the cell configuration with the lowest enthalpy per quark at each value of the pressure. In Fig. 1 we show some examples of the search for the favored cell configuration at a given pressure. We plot the ‘‘excess enthalpy per quark’’

$$\Delta h = h - h_\infty, \quad (28)$$

as a function of R , for each of the three geometries, and for various different pressures. Here h is the enthalpy per quark (16) in a given cell, and h_∞ is its value in uniform neutral quark matter *of the same pressure*. Configurations with negative Δh therefore correspond to stable mixed phases at the given pressure.

The results in Fig. 1 are for quark matter with $\mu_{\text{crit}} = 300$ MeV, $n_Q = 0.0791$ (corresponding to $m_s = 200$ MeV in (6)), and $\lambda_D = 4.82$ fm (again, a value appropriate to free quark matter with $\mu = 300$ MeV). The surface tension is 0.3 MeV/fm². The first panel of Fig. 1 shows $\Delta h(R)$ for 3D cells. The upper (red) curve is $\Delta h(R)$ at the critical pressure $p_{\text{crit}} = 1370$ MeV⁴, which is defined by the presence of a minimum with $\Delta h = 0$ (at $R \approx 10$ fm in this case). We also show $\Delta h(R)$ at a lower pressure, $p = 10$ MeV⁴; now there is a clearly favored mixed phase, with strange droplets of radius $R \approx 4$ fm. If we push the pressure down to zero then the cell size goes to infinity, and the minimum in the $\Delta h(R)$ curve moves further down to around -0.75 MeV. In the second panel we show $\Delta h(R)$ for 2D cells at the same two pressures. It

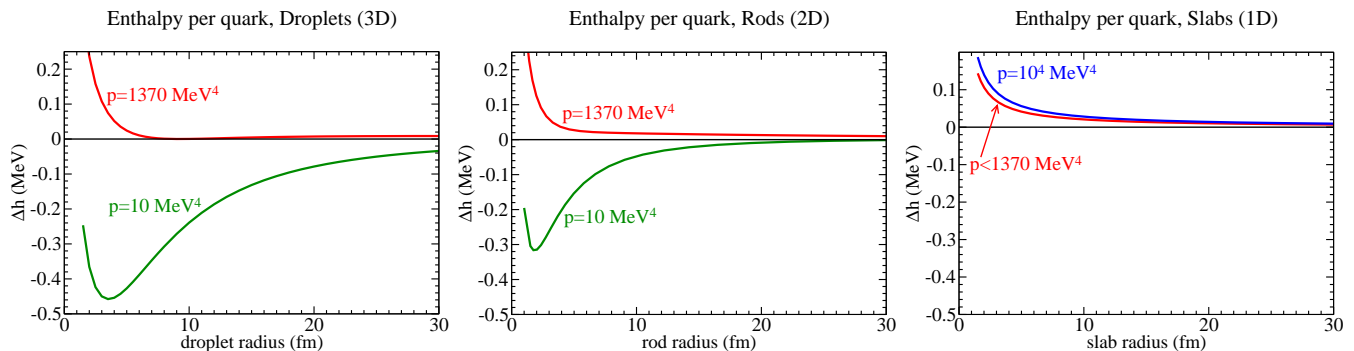


FIG. 1: Search for a stable mixed phase at different pressures. We show the excess enthalpy per quark Δh (28) as a function of the radius R of the quark matter region in the center of the cell. At each value of R , the cell radius has been chosen to give the desired pressure. The favored configuration is the one with the smallest Δh , where $\Delta h = 0$ for uniform neutral quark matter of the same pressure. For 3D cells, we find stable mixed phases (minima with negative Δh) for pressures below a critical value, $p_{\text{crit}} = 1370 \text{ MeV}^4$. 2D cells always had a higher Δh ; 1D cells were never stable. These plots are for a quark matter EoS with $\mu_{\text{crit}} = 300 \text{ MeV}$, $\lambda_D = 4.82 \text{ fm}$, $n_Q = 0.0791 \text{ fm}^{-3}$, corresponding to free quarks with a moderately heavy strange quark ($m_s = 200 \text{ MeV}$ in (6)). The surface tension was $\sigma = 0.3 \text{ MeV fm}^{-2}$.

is clear that the 2D structure has a lower critical pressure, and at these two pressures it is energetically unfavored relative to the 3D structure. In the third panel we show $\Delta h(R)$ for 1D cells. These appear to be even less favored. At $p = 1370 \text{ MeV}^4$ the $\Delta h(R)$ curve is already almost at its zero-pressure limit, which is never negative and therefore allows no mixed phase. We had to show $\Delta h(R)$ for a higher pressure, $p = 10^4 \text{ MeV}^4$, to see any change in the curve. We conclude that for this quark matter equation of state and surface tension, and at the pressures studied in Fig. 1, the only mixed phase that occurs is the 3D (droplet) one.

We note the following features of the favored configuration of the Wigner-Seitz cell:

- Increasing the pressure disfavors mixed phases: the $\Delta h(R)$ curve rises and minima are smoothed out. We hypothesize that this is because the pressure is determined by the value of μ_e at the edge of the cell (14); if $\mu_e(R_{\text{cell}})$ is increased then, because $\mu_e(r)$ is monotonic, μ_e in the quark matter is also larger (closer to μ_e^{neutral}). But this decreases the energy benefit of making a mixed phase, which arises from the departure from neutrality.
- As the dimensionality of the mixing geometry decreases from 3 to 1, mixed phases become less favored (at least in this range of pressures). We hypothesize that this is because in lower dimensional structures, a smaller proportion of the quark matter is near the surface, where μ_e is different from μ_e^{neutral} .

Since it is only the minima of $\Delta h(R)$ that are physically important, we focus on them, and in Fig. 2 we plot the value of Δh at the minimum as a function of pressure. The vertical dashed lines mark the pressures $p = 10 \text{ MeV}^4$ and $p = 1370 \text{ MeV}^4$ used in Fig. 1. We see that, for the values of the quark matter parameters studied in these figures, only droplet (3D) mixed phases will occur: slabs are never stable, and rods are never favored

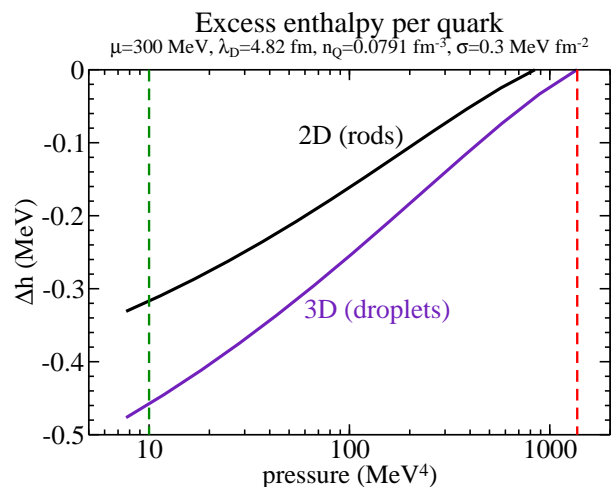


FIG. 2: Minimum value of Δh as a function of pressure, for quark matter with the same characteristics as in Fig. 1. Dashed lines mark the pressures (10 MeV^4 and 1370 MeV^4) that were used in Fig. 1. We see that for this type of quark matter the 3D (droplet) structure is always energetically favored over rods. The slab structure is never stable.

over droplets.

B. Crust thickness calculation

In Table I we show the results obtained by repeating the calculations described above for seven different quark matter equations of state and four values of the surface tension. In each case, once we have established the energetically favored configuration of the mixed phase at each pressure, we obtain the crust thickness using (1). In order to present numbers whose physical interpretation is clear, we assume that the quark star has radius

10 km and mass $1.5 M_\odot$, so we can give an explicit crust thickness in meters. From the prefactor in Eq. (1) it is easy to find the multiplicative factors that convert our values into thicknesses of crusts on stars with different masses and radii (Table II).

The first two columns of Table I specify the quark matter equation of state (2), by giving the value of n_Q and the value of λ_D (which fixes χ_Q via (5)). We fix $\mu_{\text{crit}} = 300$ MeV. The third column gives the maximum surface tension σ_{crit} for which a crust of droplets of strange matter could occur, the fourth column gives an estimated upper limit on the thickness, and the last four columns give the thickness of the crust for various values of the surface tension σ .

1. Range of parameters studied

Our assumption that the strange matter hypothesis is valid requires that μ_{crit} must be less than the quark chemical potential of nuclear matter, about 310 MeV, so we fix $\mu_{\text{crit}} = 300$ MeV. The value of μ inside our strange matter lumps will always be within a few MeV of μ_{crit} , because in order to get any crust at all the surface tension cannot be large enough to cause significant compression.

Typical values of χ_Q will be around $0.2\mu_{\text{crit}}^2$ (6), corresponding to $\lambda_D \approx 4.82$ fm. Ref. [9] found that in the 2SC phase χ_Q is smaller by a factor of 2. In Table I we explore this range, using three values, $\chi_Q = 0.2\mu_{\text{crit}}^2$, $\chi_Q = 0.1\mu_{\text{crit}}^2$, and $\chi_Q = 0.05\mu_{\text{crit}}^2$, corresponding to $\lambda_D = 4.82$ fm, $\lambda_D = 6.82$ fm, and $\lambda_D = 9.65$ fm (via (5)).

Typical values of n_Q will be around $0.05\mu_{\text{crit}}m_s^2$ (6), and a reasonable range would correspond to varying m_s over its physically plausible range, from about 100 to 300 MeV. (To have strange matter in the star, m_s must be less than μ_{crit} .) In Table I we use $n_Q = 0.0445$, 0.0791 , and 0.124 fm^{-3} , which would correspond to $m_s = 150$, 200 , and 250 MeV in (6). For $\lambda_D = 9.65$ fm we only show results for $n_Q = 0.00445 \text{ fm}^{-3}$. We do not show results for $n_Q = 0.0791 \text{ fm}^{-3}$ or $n_Q = 0.124 \text{ fm}^{-3}$, because in those cases the value of μ_e^{neutral} would be 133 MeV and 208 MeV respectively, which violates our assumption that $\mu_e \ll \mu$, and is also above the muon mass $m_\mu = 105.66$ MeV, so we would have to take into account muons as well as electrons.

The value of the maximum surface tension σ_{crit} for which a crust of droplets of strange matter could occur (third column of Table I) follows from (4). It is the maximum surface tension at which an isolated (zero-pressure) droplet would have lower enthalpy per quark than neutral quark matter at zero pressure, i.e. at the onset phase transition at $\mu = \mu_{\text{crit}}$. The last four columns of Table I give our results for the thickness of the crust at a range of values of the surface tension σ . For values of σ above σ_{crit} there is no crust. The values of σ that we use are physically reasonable, given that rough estimates of sur-

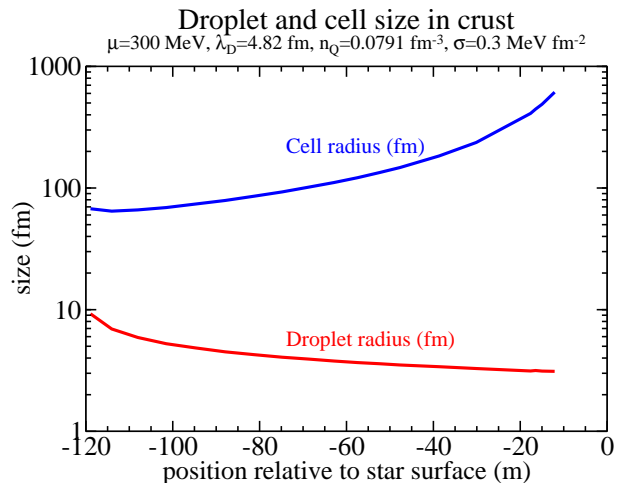


FIG. 3: Size of the quark matter droplets and the Wigner-Seitz cell (in fm) as a function of position in the the 120m-thick crust that we predict for quark matter with the stated parameter values, which correspond to free quark matter with a moderately heavy strange quark ($m_s = 200$ MeV in (6)).

face tension from the bag model are in the range 4 to $10 \text{ MeV}/\text{fm}^2$ [30, 31].

2. Crust thickness results

In Table I, we present the results of our calculation of the crust thickness as a function of the quark matter parameters. Clearly the thickness is very sensitive to the values of these parameters.

In Table II we give the correction factors for some typical masses and radii that are expected for quark stars (see, for example, Ref. [3], Fig. 28). We see that smaller and lighter quark stars have thicker crusts. In fact, for a star of radius 4 km [32] the crust thickness could easily be of order 1000 m, at which point the assumption $\Delta R/R_{\text{star}}$ used in Eq. (1) begins to become questionable. If the crust is thick enough then one must keep higher powers of $\Delta R/R_{\text{star}}$ in calculating it, and it may even be necessary to solve the full Tolman Oppenheimer Volkoff equation [17, 18].

Some of the crust thicknesses in Table I are given as lower limits. This is because for large λ_D and n_Q , and low surface tension, mixed phases are highly favored, and persist up to extremely high pressures (of order 10^6 MeV^4). To achieve such a high pressure requires a very “cramped” cell geometry, in which R_{cell} is only a little larger than the quark droplet radius R . In such a geometry we can no longer trust our approximation of treating the cell as spherical, rather than a unit cell of a crystal lattice (e.g. cubic). We therefore use an alternative upper limit p_{max} on the pressure: p_{max} is the pressure below which the favored cell configuration always has $R_{\text{cell}} > 2R$. We can then calculate a lower limit on the crust thickness, by integrating (1) up to p_{max} .

λ_D (fm)	n_Q (fm ⁻³)	$\sigma_{\text{crit}}(3D)$ (MeV fm ⁻²)	ΔR_{max} (m)	ΔR (m) at			
				$\sigma=0.3$	$\sigma=1.0$	$\sigma=3.0$	$\sigma=10.0$
4.82	0.0445	0.533	36	9	–	–	–
4.82	0.0791	1.69	120	67	25	–	–
4.82	0.124	4.12	280	220	160	39	–
6.82	0.0445	1.51	72	40	13	–	–
6.82	0.0791	4.8	230	> 170	120	45	–
6.82	0.124	11.6	550	> 460	> 390	280	39
9.65	0.0445	4.27	140	110	75	22	–

TABLE I: Crust thickness ΔR (in meters) for a strange star of radius 10 km and mass $1.5 M_\odot$; for more general stars see Table II. We calculate the crust for seven different quark matter equations of state and four values of the surface tension. The first two columns, λ_D and n_Q , specify the quark matter equation of state (2) (via (5)). The third column gives the maximum surface tension for which a strangelet crust will occur (4). The fourth column gives a rough upper limit on ΔR using an estimate from Ref. [8]. The last four columns give our results for the crust thickness in meters for different values of the surface tension σ (given in MeV fm⁻²) of the interface between quark matter and vacuum. The crust thickness is very sensitive to the equation of state and the surface tension. It ranges from zero up to several hundred meters.

R (km)	M (M_\odot)	$\Delta R/(\Delta R \text{ in Table I})$
4	0.05	8.3
6	0.2	4.4
8	0.5	2.8
10	1.0	2.0

TABLE II: Correction factors to be applied to crust thickness values in Table I, for quark stars of various radii and masses. These follow from the factor multiplying the integral in Eq. (1). Note that smaller stars have thicker crusts.

In the limit of low surface tension, our results are compatible with the upper limit ΔR_{max} (fourth column in Table I) which follows from taking the estimate obtained by ignoring surface tension and Debye screening in Ref. [8] (their Eq. (13)) and applying the TOV correction factor $(1 - 2GM/R_{\text{star}})$. We find that even a relatively moderate surface tension, around 1 to 10 MeVfm⁻², reduces the thickness of the crust or even eliminates it completely. The mechanism is clear: larger values of the surface tension disfavor the mixed phase by increasing surface energy costs, leading to a lower p_{crit} and thinner crusts. However, it remains possible that a quark star could have a crust hundreds of meters thick.

We find that the crust is thickest for large values of n_Q and λ_D , as one would expect from the estimate $\Delta R_{\text{max}} \propto n_Q^2/\chi_Q \propto n_Q^2 \lambda_D^2$ [8]. This is consistent with the observation from Fig. 1 that we can measure how favored a mixed phase is by the depth Δh_{min} of the minimum in $\Delta h(R)$. Since the $\Delta h(R)$ curve moves up as the pressure increases (see Sec. V A), we can guess that the deeper the minimum at zero pressure, the thicker the crust. From Ref. [9] (Fig. 2 and Eq. (26)), we find that at a given σ , the depth of the minimum is $\Delta h_{\text{min}} \propto -n_Q^2/\chi_Q$, i.e. $\Delta h_{\text{min}} \propto -n_Q^2 \lambda_D^2$. Hence the mixed phase is more favored, and the crust is thicker, for larger values of n_Q and λ_D .

All the crusts in Table I consist entirely of 3D structures, i.e. spherical droplets of quark matter in a neutral-

izing background of electrons. We never found any pressure for any quark matter parameters where 2D (rod) or 1D (slab) structures were energetically preferred. It would be interesting to see whether this remains true when the cell is allowed to be a different shape from the strangelet (e.g. square or cubic cells).

3. Internal structure of the crust

In Fig. 3 we select one of our quark matter equations of state, and show how the properties of the strangelet crystal lattice vary with position in the crust. The horizontal axis is $\Delta r = r - R_{\text{star}}$, so more negative values correspond to deeper parts of the crust. The plot should end at $\Delta r = 0$, but we were not able to push our numerical calculations to that value, so the curves end at $\Delta r \approx -10$ m.

As one approaches the surface, the size R_{cell} of the Wigner-Seitz cell grows very large (note that Fig. 3 uses a logarithmic scale for the vertical axis). This means that the strangelet density becomes very low. We expect that as $\Delta r \rightarrow 0$, R_{cell} will diverge, since the pressure must go to zero, so μ_e at the edge of a cell must go to zero, so the cell size must become infinite. In this limit the droplets in the crust effectively become isolated strangelets, and we expect their size to settle down to that of the most stable isolated strangelet for this form of quark matter. We can predict this value from Ref. [9], eqn (24): by minimizing the free energy per quark $\Delta g/n$ (which is equivalent to Δh in this paper) for the values of μ_{crit} , n_Q , χ_Q , and σ used in Fig. 3, we find that the most stable strangelet has a radius of 3.0 fm, which is exactly the asymptotic value emerging in Fig. 3. For such small strangelets we expect that our Thomas-Fermi approach is not accurate, and shell model corrections will become important: including such corrections is a topic for future research.

As one goes deeper into the star (Δr becoming more negative), the pressure rises, so the cell size decreases, and the droplet size slowly increases, until we reach the

critical pressure at which uniform neutral quark matter becomes favored over the strangelet lattice. This is a first-order phase transition, as is clear from Fig. 1, so the curves in Fig. 3 end suddenly, without any singular behavior. In this paper we do not take in to account the possibility of a metastable lattice that might persist to higher pressures.

Fig. 3 shows that the strangelet crystal crust of a quark star tends to be fairly dilute: over most of the crust the quark matter droplet size is small, of order the Debye length in quark matter λ_D , while the cell size is larger, by a factor of 10 or more.

VI. DISCUSSION

The calculations described in this paper give us a more precise picture of the strangelet-crystal crust of a quark star. The results presented in Table I show that the thickness of the strangelet-crystal crust of a strange star is very sensitive to the surface tension σ of the interface between quark matter and the vacuum, and to the quark matter parameters n_Q and χ_Q (2), which determine the response of the quark matter to deviations of the electrostatic potential from its neutrality value. Our results are compatible with those of Ref. [8] where an upper limit on the crust thickness was obtained by ignoring surface tension and Debye screening. The crust is thickest for large n_Q and small χ_Q (large λ_D). As discussed in Sec. VB2, we find that values of surface tension in the physically expected range, around 1 to 10 MeVfm⁻², reduce the thickness of the crust and may even eliminate it completely, but it remains possible that a quark star of radius 10 km could have a crust several hundred meters thick. From Table II we see that for a smaller star the crust could be even thicker.

The geometry of the mixed phase in our crusts, on the other hand, shows no variation at all. It is always three-dimensional, containing spherical droplets of quark matter. We never find any case where a two-dimensional (rod) or one-dimensional (slab) geometry is favored.

Our calculations and results suggest two directions for future work: firstly, one could study phenomenological consequences of our understanding of the strangelet-crystal crust of a quark star. Secondly, one could improve on our treatment of the strangelet crystal, by relaxing some of the assumptions listed in Sec. I.

The most obvious phenomenological task is to revisit computations of the frequencies of seismic vibrations which are observed after giant flares in magnetars [33, 34]. Ref. [33] found that the strangelet crystal crust did not have the right spectrum of toroidal shear modes to account for current observations: it would be interesting to see whether taking in to account the surface tension and Debye screening affects that conclusion. Other aspects of the phenomenology of the crust could also be studied, for example (a) the thermal response of the crust to accretion [35]; (b) the role of the crust in the trapping

of neutrinos and photons just after a type-II supernova [36]; (c) the spectrum of photons radiated from the surface of a quark star [37, 38, 39]; (d) the contribution of the crust to the moment of inertia and glitches [40]; (e) the damping of r -modes in by shear viscosity in the crust [41, 42] (for quark stars, the contribution from the interior has been calculated [43, 44]); (f) the thermal relaxation time of the crust and its response to the post-supernova “cooling wave” [45]. The thermal relaxation time of the crust depends on the thermal conductivity, for which we can make a very rough estimate using appendix A of Ref. [45]. We find values of order a few hundred MeV² at $T \sim 0.1$ MeV, which is comparable to the range 10^{18} erg cm⁻¹s⁻¹K⁻¹ for low-density nuclear matter (Ref. [45], Fig. 4). We defer a more accurate calculation to future work.

To improve on our treatment, the most pressing issues are to use a realistic shape for the Wigner-Seitz cells (which should be unit cells of some regular lattice, rather than spheres), to include shell-model corrections for the smallest strangelets, and to allow for “Swiss-cheese” phases where most of the unit cell consists of quark matter, with a hole at the center containing electrons.

As discussed in Sec. VB2, the shape of the cell becomes important at very high pressures, and our use of the spherical approximation meant that in some cases we could only obtain lower limits on the crust thickness. Studying more realistic shapes is straightforward in principle, but would require a more demanding multidimensional numerical solution of the Poisson equation.

Shell-model corrections can be of order one MeV per quark for strangelets of size $R \lesssim 5$ fm [20, 21], which is not negligible relative to our typical enthalpy per quark (Fig. 1), and may therefore affect our results for the outer part of the crust, where we predict strangelets as small as 3 fm (Fig. 3).

Treating Swiss-cheese phases would require us to include curvature energy as well as surface tension. This highlights the fact that we treated the interface between quark matter and vacuum in a very simplified way, as a zero-width interface with a surface tension. However, since the quark confinement distance is about 1 fm, the interface might well have structure on this distance scale. Like the shell-model effects described above, this could be relevant to the low-pressure regime, where the strangelets can be as small as a few fm. There are even indications that when such physics is taken into account, the CFL phase may undergo some degree of charge separation [23, 25], raising the possibility that there might be some sort of crystalline crust on quark stars made of CFL quark matter.

Acknowledgments

We thank Junhua Chen, Prashanth Jaikumar, Jes Madsen, Sanjay Reddy for useful discussions. This re-

search was supported in part by the Offices of Nuclear Physics and High Energy Physics of the Office of Science of the U.S. Department of Energy under contracts #DE-FG02-91ER40628, #DE-FG02-05ER41375, and by

the Undergraduate Research Office and McDonnell Center for Space Sciences of Washington University in St. Louis.

-
- [1] A. R. Bodmer, Phys. Rev. **D4**, 1601 (1971).
 [2] E. Witten, Phys. Rev. **D30**, 272 (1984).
 [3] F. Weber, Prog. Part. Nucl. Phys. **54**, 193 (2005), [astro-ph/0407155].
 [4] E. Farhi and R. L. Jaffe, Phys. Rev. **D30**, 2379 (1984).
 [5] C. Alcock, E. Farhi and A. Olinto, Astrophys. J. **310**, 261 (1986).
 [6] M. Stejner and J. Madsen, Phys. Rev. **D72**, 123005 (2005), [astro-ph/0512144].
 [7] V. V. Usov, Astrophys. J. **481**, L107 (1997), [astro-ph/9703037].
 [8] P. Jaikumar, S. Reddy and A. W. Steiner, Phys. Rev. Lett. **96**, 041101 (2006), [nucl-th/0507055].
 [9] M. G. Alford, K. Rajagopal, S. Reddy and A. W. Steiner, Phys. Rev. **D73**, 114016 (2006), [hep-ph/0604134].
 [10] M. G. Alford, J. A. Bowers and K. Rajagopal, Phys. Rev. **D63**, 074016 (2001), [hep-ph/0008208].
 [11] R. Casalbuoni and G. Nardulli, Rev. Mod. Phys. **76**, 263 (2004), [hep-ph/0305069].
 [12] D. G. Ravenhall, C. J. Pethick and J. R. Wilson, Phys. Rev. Lett. **50**, 2066 (1983).
 [13] M. G. Alford, A. Schmitt, K. Rajagopal and T. Schafer, 0709.4635.
 [14] H. Heiselberg, Phys. Rev. **D48**, 1418 (1993).
 [15] N. K. Glendenning, Phys. Rev. **D46**, 1274 (1992).
 [16] M. Alford, C. Kouvaris and K. Rajagopal, Phys. Rev. **D71**, 054009 (2005), [hep-ph/0406137].
 [17] R. C. Tolman, Phys. Rev. **55**, 364 (1939).
 [18] J. R. Oppenheimer and G. M. Volkoff, Phys. Rev. **55**, 374 (1939).
 [19] T. Maruyama, S. Chiba, H.-J. Schulze and T. Tatsumi, Phys. Rev. **D76**, 123015 (2007), [0708.3277].
 [20] J. Madsen, Phys. Rev. **D50**, 3328 (1994), [hep-ph/9407314].
 [21] P. Amore, M. C. Birse, J. A. McGovern and N. R. Walet, Phys. Rev. **D65**, 074005 (2002), [hep-ph/0110267].
 [22] J. Madsen, Phys. Rev. Lett. **85**, 4687 (2000), [hep-ph/0008217].
 [23] J. Madsen, Phys. Rev. Lett. **87**, 172003 (2001), [hep-ph/0108036].
 [24] J. Madsen, Phys. Rev. Lett. **100**, 151102 (2008), [0804.2140].
 [25] M. Oertel and M. Urban, Phys. Rev. **D77**, 074015 (2008), [0801.2313].
 [26] M. B. Christiansen and N. K. Glendenning, Phys. Rev. **C56**, 2858 (1997), [astro-ph/9706056].
 [27] M. B. Christiansen and J. Madsen, J. Phys. **G23**, 2039 (1997).
 [28] Y. Lyubarsky, D. Eichler and C. Thompson, Astrophys. J. **580**, L69 (2002), [astro-ph/0211110].
 [29] E. W. Weisstein, Jacobi elliptic functions., From MathWorld—A Wolfram Web Resource. <http://mathworld.wolfram.com/JacobiEllipticFunctions.html>.
 [30] M. S. Berger and R. L. Jaffe, Phys. Rev. **C35**, 213 (1987).
 [31] M. S. Berger and R. L. Jaffe, Phys. Rev. C **44**, 566 (1991).
 [32] E. S. Fraga, R. D. Pisarski and J. Schaffner-Bielich, Phys. Rev. **D63**, 121702 (2001), [hep-ph/0101143].
 [33] A. L. Watts and S. Reddy, Mon. Not. Roy. Astron. Soc. **379**, L63 (2007), [astro-ph/0609364].
 [34] A. I. Chugunov, Mon. Not. Roy. Astron. Soc. **371**, 363 (2006), [astro-ph/0606310].
 [35] E. F. Brown, Astrophys. J. **531**, 988 (2000), [arXiv:astro-ph/9910215].
 [36] A. Burrows, S. Reddy and T. A. Thompson, Nucl. Phys. **A777**, 356 (2006), [astro-ph/0404432].
 [37] D. Page and V. V. Usov, Phys. Rev. Lett. **89**, 131101 (2002), [astro-ph/0204275].
 [38] P. Jaikumar, C. Gale, D. Page and M. Prakash, Int. J. Mod. Phys. **A19**, 5335 (2004), [astro-ph/0407091].
 [39] T. Harko and K. S. Cheng, Astrophys. J. **622**, 1033 (2005), [astro-ph/0412280].
 [40] N. K. Glendenning and F. Weber, Astrophys. J. **400**, 647 (1992).
 [41] L. Bildsten and G. Ushomirsky, Astrophys. J. Lett. **529**, L33 (2000), [arXiv:astro-ph/9911155].
 [42] O. L. Caballero, S. Postnikov, C. J. Horowitz and M. Prakash, 0807.4353.
 [43] J. Madsen, Phys. Rev. Lett. **85**, 10 (2000), [astro-ph/9912418].
 [44] P. Jaikumar, G. Rupak and A. W. Steiner, 0806.1005.
 [45] O. Y. Gnedin, D. G. Yakovlev and A. Y. Potekhin, Mon. Not. Roy. Astron. Soc. **324**, 725 (2001), [astro-ph/0012306].